Negative interactions and virulence differences drive the dynamics in multispecies bacterial infections

Désirée A. Schmitz[a], Richard C. Allen[a] & Rolf Kümmerli[a]

[a] Department of Quantitative Biomedicine, University of Zurich, Winterthurerstrasse 190, 8057 Zurich, Switzerland

Correspondence to: desiree.schmitz@uzh.ch or rolf.kuemmerli@uzh.ch

Competing interests statement: The authors declare that they have no conflict of interests. Funding for this project comes from the Swiss National Science Foundation (grant no. 31003A_182499 to RK) and from the Novartis Foundation for Medical-Biological Research (to RK).

Abstract

Bacterial infections are often polymicrobial, leading to intricate pathogen-pathogen and pathogen-host interactions. There is increasing interest in studying the molecular basis of pathogen interactions and how such mechanisms impact host morbidity. However, much less is known about the ecological dynamics between pathogens and how they affect virulence and host survival. Here we address these open issues by co-infecting larvae of the insect model host *Galleria mellonella* with one, two, three or four bacterial species, all of which are opportunistic human pathogens. We found that virulence was always driven by the most virulent species regardless of the number of species and pathogen combinations injected. Moreover, we observed a link between a pathogen's virulence and its growth within the host. In certain cases, the more virulent pathogen simply outgrew the less virulent pathogen. In other cases, we found evidence for negative interactions between pathogens inside the host, whereby the more virulent pathogen typically won a competition. Taken together, our findings reveal positive links between a pathogen's growth inside the host, its competitiveness towards other pathogens, and its virulence. Beyond being generalizable across species combinations, our findings suggest that treatment strategies against polymicrobial infections should target the most virulent species.

Introduction

Research over the past decades has revealed that many bacterial infections are polymicrobial [1]–[4] . This can lead to complicated pathogen-pathogen and pathogen-host interactions. The ecological interactions between pathogens can range from competition through commensalism to cooperation, and such interactions can have consequences for the host [5]. For example, mutually beneficial cross-feeding between a human commensal bacterium and a pathogen was shown to increase the virulence of the latter, thus exacerbating host morbidity [6]. Competition can also enhance virulence as revealed for the pathogen *Pseudomonas aeruginosa* which increases the production of the toxin pyocyanin that harms both its competitor *Staphylococcus aureus* and host tissue [7]. Interaction patterns can become even more complex in chronic infections, where (co-)evolution can occur between pathogens and between pathogens and the host [8]–[13]. There is increasing awareness that such eco-evolutionary dynamics affect host health and are important to consider regarding treatment options [5].

For this reason, research on interactions between pathogenic bacteria has flourished in the past years. For example, there is a wealth of work on interactions between *P. aeruginosa and S. aureus*, two of the most troublesome nosocomial pathogens [14]–[16]. This research, often carried out *in vitro*, has successfully identified molecular mechanisms of pathogen interactions and evolutionary patterns of how pathogens adapt to one another. However, we know much less about pathogen-pathogen interactions within hosts and how interactions drive virulence. Moreover, it is often unclear whether insights from a particular pathogen pair are generalizable and hold for other pathogen and strain combinations [17].

Here, we aim to tackle these questions by studying bacterial interactions between four different opportunistic human pathogens in an insect host, the larvae of the greater wax moth *Galleria mellonella*. This model host is suitable for our purpose because it allows for relatively high-throughput experiments where many different pathogen combinations can be tested, and well-defined doses of pathogens can be injected into a larva. Moreover, *G. mellonella* has an innate immune system that resembles the vertebrate innate immune response and lives approximately at human body temperature, which makes it an excellent model organism to study human bacterial pathogenesis [18]–[21]. Regarding pathogens, our aim was to choose phylogenetically distinct species that are likely to exhibit different levels of virulence. We picked the following four opportunistic human pathogens. *Pseudomonas aeruginosa* (P) is a species of high clinical relevance that causes a number of both community- and hospital-acquired infections including skin and wound infections, urinary tract infections, bloodstream infections, and pneumonias [22], [23]. *Burkholderia cenocepacia* (B) causes chronic lung infections in immunocompromised patients, e.g. suffering from cystic fibrosis [24]. *Klebsiella michiganensis* (K) belongs to the *K. oxytoca* complex [25], which are human pathogens that lead to health care-associated infections as well as to a variety of infections such as diarrhea, bacteremia, and meningitis [26]–[28]. *Cronobacter sakazakii* (C) can also cause bacteremia and meningitis as well as necrotizing enterocolitis and brain abscess/lesions [29]. While some of these pathogens can be found together – P and B in lung infections of cystic fibrosis patients [4], [30], [31] and P and K in burn wound infections [32], [33] – others might not naturally co-occur in an infection. However, natural co-occurrence is not the focus of our work. Instead, we aim to derive general principles of how different pathogens interact within the host and how this affects host survival.

82 In a first set of experiments, we aimed to understand the demographics of
83 pathogen-host interactions in single species (mono) infections. For this purpose, we
84 manipulated the injection dose and host age to understand how these factors affect
85 each pathogen's virulence for the host. Second, we conducted mixed species infection
86 experiments (double, triple, and quadruple) to assess how polymicrobial infections
87 affect virulence patterns and host survival. Third, we enumerated pathogen growth
88 within the host at two time points for all mono and pairwise infections to test whether
89 pathogen load links to virulence. Fourth, we followed changes in pathogen frequencies
90 in mixed infections to derive pathogen interaction patterns. While this approach does
91 not reveal specific molecular mechanisms of pathogen interactions, it allows us to
92 distinguish between negative, neutral, and positive interactions between co-infecting
93 pathogens and how such interactions link to virulence.

Material and Methods

Bacterial strains & host

We used the following four opportunistic human pathogens: *Pseudomonas aeruginosa* PAO1 [34], *Burkholderia cenocepacia* K56-2 [35], *Klebsiella michiganensis*, and *Cronobacter sakazakii* (ATCC29004). We purchased the larvae of the greater wax moth *G. mellonella* in their last instar stage from a local vendor (Bait Express GmbH, Basel, Switzerland). Upon arrival, we stored them at 4-8° C without food. We considered larval age as the number of days after arrival in our laboratory, since the exact age of larvae was unknown to us. When examining larval age, we compared larvae that were ordered at the same time (i.e., same batch), but were infected at different time points.

Culturing conditions of bacteria

Bacterial stocks were kept in 25% glycerol and stored at -80° C. For all experiments, we grew bacteria overnight until stationary phase in 5 mL lysogeny broth (LB) in 50 mL Falcon tubes at 37° C and at 170 rpm with aeration (Infors HT, Multitron Standard Shaker). For all species, we centrifuged 1 mL overnight-cell culture in a 1.5 mL Eppendorf tube at 7'500 rcf for 5 min (Eppendorf, tabletop centrifuge MiniSpin plus with rotor F-45-12-11) and washed cultures three times with a 0.8% NaCl solution to remove all original media. Next, we measured the optical density at 600 nm (OD_{600}) of the washed cell culture (Amersham Biosciences, Ultrospec 2100 pro spectrophotometer), adjusted it to OD_{600}=1, and diluted each species individually to obtain similar cell numbers per milliliter for all species. All chemicals were purchased from Sigma Aldrich, Switzerland, unless indicated otherwise.

120 **Infection procedure**

121 We sorted larvae and evenly distributed them across treatments according to size.
122 Their weight ranged from 278-731 mg with an average weight of 499 mg. We put larvae
123 on ice in a petri dish to immobilize them. Next, we surface-sterilized larvae with 70%
124 ethanol and injected them between the posterior prolegs. We used a sterile hypodermic
125 needle (Braun, 0.45 x 12 mm BI/LB, 26G), a sterile syringe (Braun, 0.01-1 mL Injekt-F
126 Luer Solo), and a programmable syringe pump (New Era Pump Systems Inc, model
127 NE-300) to standardize injection speed. With a flow rate of 2 ml/h, we either injected
128 10 µL control or bacterial solution (both in 0.8 % NaCl) into larvae within 18 s. We had
129 a second control treatment, where larvae were not injected. The injection dose ranged
130 from 10^2 to 10^6 CFU for mono infections and was kept at 10^5 CFU for experiments that
131 included multispecies infections. In multispecies infections, we mixed equal amounts
132 of each species. For all experiments, we confirmed the injection dose in triplicate by
133 counting colony forming units (CFU) on 1.5% LB agar plates. We distributed injected
134 larvae to individual wells of a 12-well plate for incubation at 37° C in the dark without
135 food. We monitored survival of every larva in regular intervals (hourly during 12-24
136 hours post infection (hpi) and every two hours during 36-48 hpi). Larvae were
137 considered dead when they did not move upon touch with a pipette tip.

138

139 **Bacterial load in the hemolymph**

140 We determined the bacterial load in all larvae that received mono-, mixed-, NaCl, and
141 no infection at two time points, at 6 and 12 hpi. Since larvae had to be sacrificed during
142 this process, we had two independent batches of larvae that were used for the
143 respective timepoints. First, we placed larvae individually in 2 mL Eppendorf tubes and
144 submerged those in ice until larval movement halted. Then, we opened each larva with
145 a surgical blade (Aesculap AG, Germany) behind the posterior prolegs, with the cut

146 length spanning half of the body width. We sterilized the blade with 70% ethanol
147 between different larvae. Next, we drained the hemolymph into a fresh 1.5 mL
148 Eppendorf tube by gently squeezing the larva. The collected hemolymph was mixed
149 and stored on ice. To enumerate bacterial CFU, we serially diluted 10 µL of the
150 collected hemolymph in 0.8% NaCl up to 10^{-6} and plated the appropriate dilutions on
151 LB-agar plates (1.5% agar) in duplicates. The appropriate dilutions varied between 10^{0}
152 (undiluted) and 10^{-6} and depended on the bacterial species. We incubated the plates
153 at 37° C overnight and then manually counted CFU. Because *B. cenocepacia* grew
154 slower than the other species, plates were incubated for two days. Plates with *C.*
155 *sakazakii* were kept at room temperature for an additional day following overnight
156 incubation for colonies to develop their characteristic yellow color. All four species
157 could be distinguished from each other based on their different colony morphologies
158 (see Fig. S3 in the supplemental information). We considered plates with a minimum
159 of 25 CFU up to a number of CFU for which we could still distinguish single colonies
160 with confidence. Plates with less than 25 CFU were only considered if none of the
161 plated dilutions from the same individual adhered to this threshold. For mixes where
162 one species occurred at very low frequency (mostly mixes with P), we plated the
163 undiluted hemolymph to see whether the rare species was present at all. While both C
164 and K were visible even in a lawn of P, this was not true for B. For this species
165 combination, we cannot conclude that B was completely absent in certain larvae but
166 rather that P was highly dominant. We calculated the CFU/larva by multiplying the
167 volume of plated hemolymph with the average larval weight since larval weight is
168 almost identical to larval liquid volume according to Andrea et al. [36].
169
170 In approximately 20% of the extracted larval hemolymph, we detected bacteria
171 different from our four focal species. While the presence of other microbes can be

172 expected, we excluded these larvae from further analysis as it was unclear whether
173 these bacteria represent other pathogens or are part of the natural microbiome of
174 larvae. Nonetheless, we determined the identity of ten representative isolates by 16S
175 rRNA sequencing (colony PCR using standard primers 1492r and 27f). We identified
176 *Enterococcus casseliflavus*, and *E. gallinarum*, two common insect gut bacteria [37],
177 [38], as the closest relatives of our isolates with sequence identities of 89-99%.
178

179 **Statistical analysis**

180 All statistical analyses were performed with R (version 4.1.1) and the interface RStudio
181 (version 2021.09.0) [39]. For the dose-response curves in Fig. 1A, we measured mean
182 survival time of the host as the area under the full survival curve using the function
183 survmean from the survival package [40]. To build a log-logistic model we used the
184 drm function from the drc package [41]. To compare host survival in mono versus
185 mixed infections, we built a separate model for each panel shown in Fig. 2, comparing
186 host survival of a particular pathogen combination. The statistical results were robust
187 across three different methods comparing host survival: the non-parametric Log-rank
188 test, the semi-parametric Cox proportional hazards model, and the parametric Weibull
189 regression. See Table S1 for a model comparison.

190 To determine whether the pathogens significantly vary in their bacterial load in
191 mono infections, we compared the CFU extracted from the hemolymph of host
192 individuals at 6 hpi and 12 hpi. We chose a linear model using generalized least
193 squares to account for differences in variance between the species, which was mainly
194 caused by *K. michiganensis* at 12 hpi (see Table S3 for the full statistical analysis).
195 Next, we performed a post-hoc analysis using the Tukey honest significant difference
196 test with p-value adjustment to compare the bacterial load between species.

To compare bacterial load in the hemolymph in mono- versus mixed infections, we built a separate linear model for each pathogen to test whether its growth was influenced by the presence of another species, the CFU of this other species and time (at 6 hpi versus 12 hpi). Since the injection dose was always the same independent of how many species were injected, we compared for each species half the CFU found in mono infections to the total CFU (for the focal species) observed in pairwise infections. To obtain normally distributed residuals, we transformed all CFU values in our models. We used the function transformTukey from the rcompanion package to find the best transformation [42]. Non-significant interaction terms and main effects were removed from models until a minimal model was obtained. Most of the minimal models included both a main effect of the coinfecting species and its CFU effect. We often found that these two explanatory variables had opposing signs, which means that the influence of the co-infecting species on the focal species depended on the actual CFU of the coinfecting species. For this reason, we assessed the threshold CFU of the co-infecting pathogen at which its effect on the focal pathogen switches from being positive to being negative. This was done for each pathogen combination. We could then compare this CFU threshold to our experimental CFU values to check whether a coinfecting species stimulated or inhibited a focal species. To calculate the standard error for confidence intervals of this threshold and the p-value (one sample t-test versus zero) we used the Taylor expansion in the R package propagate [43].

Results

Injection dose, host age, and species identity determine virulence

To assess how the four different pathogens affect host survival, we exposed different age classes of *G. mellonella* larvae (5 - 15 days old prior to experimentation) to a range of pathogen injection doses (100 to 1 million colony forming units, CFU) for each of the four pathogens (B, C, K, P) and tracked their survival over 48 hours (Fig. 1A and 1B).

We found that the hazard to die differed between the four species (Cox proportional hazard: χ^2_3 = 308.6, p < 0.0001) and was influenced by significant interactions between species and larval age (χ^2_3 = 67.28, p < 0.0001), and species and injection dose (χ^2_3 = 10.96, p = 0.0119). When examining these interactions more closely, we observed that the hazard to die grew significantly with increasing larval age for C (z = 2.69, p = 0.0071) and K (z = 6.43, p < 0.0001), but only marginally for B (z = 1.90, p = 0.0573), and not at all for P (z = -0.72, p = 0.471). For the injection dose, we found that higher CFU significantly increased the hazard to die in all four species, but the hazard increase was more pronounced for B and P than for K and C (see Table S1 for the full statistical analysis). The reason for the species-specific relationship between virulence and infection dose stems from the fact that the survival decreased in a log-linear fashion for B and P with higher pathogen doses, whereas C and K only became virulent above a certain threshold injection dose of about 10^4 CFU for K and 10^5 CFU for C.

Based on the insights from this experiment, we decided to use an injection dose of 10^5 CFU for all subsequent experiments. At this injection dose, all four pathogens are virulent with the following order of virulence: *P. aeruginosa* (P) > *B. cenocepacia* (B) > *K. michiganensis* (K) > *C. sakazakii* (C), and with significant host age effects for C and K (Fig. 1C).

243 **Virulence dynamics of multispecies infections are driven by the most virulent**
244 **species**

245 Next, we compared host survival between mono and mixed infections. For this, we
246 injected pairwise combinations of our four bacterial species into larvae of *G. mellonella*
247 and observed their survival over 48 h (Fig. 2A). The injection dose was always 10^5
248 CFU in total, with equal amounts of each co-injected species. An intuitive expectation
249 is that the virulence in coinfections should be intermediate between the mono
250 infections of the two species. In contrast to this expectation, we found that any mixed
251 infection followed the dynamics of its most virulent species (Fig. 2B). A statistical
252 examination confirmed that larval survival was not different between the mixed
253 infection and the mono infection of the more virulent species in three out of six cases
254 (Log-rank test B+K vs. B: $p = 0.2459$; C+K vs. K: $p = 0.9770$; C+P vs. P: $p = 0.0548$).
255 In the remaining three cases, survival in the mixed infection was significantly lower
256 than the mono infection of the more virulent species (B+C vs. B: $p = 0.0033$; B+P vs.
257 P: $p = 0.0230$; K+P vs. P: $p = 0.0041$), but the actual biological differences observed
258 are extremely small (Fig. 2B).

259 We then tested whether the same patterns arise in the four triple and the
260 quadruple infections. As above, we kept the total number of CFU constant at 10^5 CFU
261 and mixed equal amounts of each pathogen. As for the paired infections, we found that
262 the survival trajectory of larvae infected with three and four pathogens followed the
263 trajectories of the mono infection of the most virulent species in the mix (Fig. 2C). For
264 example, in the triple infection with B, C, and K, larval survival followed the one of the
265 B mono-infection, which is the most virulent of the three species. In the remaining four
266 mixes, the most virulent species was P and in all these cases larval survival followed
267 the one of P mono infections. Statistical analyses revealed subtle but significant
268 differences: mixed infections with P were always slightly less virulent than the mono

269 infections with P (see Table S2 for the full statistical analysis). We can explain this
270 pattern by a density effect: fewer P cells were injected in higher order infections, and
271 thus bacteria needed more time to replicate and reach sufficient numbers to kill the
272 larval host.

The most virulent species is also more abundant both in mono and mixed infections

We then asked what the underlying reason could be for our observation that the most virulent species drives host survival dynamics. One explanation would be that the more virulent species grows better in the host, making it more abundant and thereby exerting a stronger effect on the host. We tested this hypothesis in mono infections first and found that bacterial load (CFU per larva) of the four pathogens followed the exact order of their virulence at 12 hours post infection (hpi, see Fig. S2 in the supplemental information, and Table S3 for the full statistical analysis). At the earlier timepoint (6 hpi), the same pattern holds for B, C, and P, whereas K had much higher CFU inside the host than expected from its virulence. The data imply that K initially grows well in larvae, while it is compromised later during the infection. Overall, the mono infection data suggest that pathogen load in a host positively links to its level of virulence (i.e., negatively with host survival).

Next, we explored whether the same is true for mixed infections, i.e., whether the dominant effect of the more virulent species might be caused by its higher abundance in a coinfection. Indeed, in all cases the more virulent species was also the more abundant species at 12 hpi (Fig. 3). For example, P as the most virulent of our pathogens dominated in terms of abundance in all larvae in any of its mixes at 12 hpi. However, we also found evidence for more complex dynamics, where relative species abundance changed over time. Especially in the infection pairs K+P and K+B, we observed that K dominated at 6 hpi despite being the less virulent species, a pattern that disappeared at 12 hpi. Important to note is that in five out of six pairings both pathogen species coexisted in the host during the course of the infection in a large proportion of larvae.

299 **Negative interactions dominate in pairwise infections**

300 We used the CFU data from mixed infections to test whether the growth of any of the
301 four species was influenced by the presence of a coinfecting species across two time
302 points (at 6 and 12 hpi). We found that the coinfecting species had either no effect or
303 a negative effect on a focal species in a pathogen-pair specific way (Fig. 4, see Table
304 S4 for the full statistical analysis). The negative effect was either independent of how
305 prevalent the coinfecting species was (main effect) or stronger with increasing CFU of
306 the coinfecting species (CFU effect).

307 *B. cenocepacia* (B): The growth of this pathogen increased from 6 hpi to 12 hpi
308 (t_{77} = 2.66, p = 0.0095), and was not affected by C (t_{77} = -0.10, p = 0.9171). In contrast,
309 B growth was compromised by increasing numbers of K at the earlier timepoint and P
310 at both timepoints (CFU effect of second species, for K: t_{77} = -4.73, p < 0.0001; for P:
311 t_{77} = -4.17, p < 0.0001). The presence of P at 12 hpi resulted in a CFU drop of B even
312 below the inoculum size in many larvae.

313 *C. sakazakii* (C): In mono infections, this pathogen's CFU dropped below the
314 inoculum size for both timepoints, suggesting that it cannot replicate within the host.
315 While the presence of B did not affect C at any given time, both K and P significantly
316 compromised C abundance (main effect, for K: t_{66} = -3.29, p = 0.0016; for P: t_{66}= -2.20,
317 p = 0.0314).

318 *K. michiganensis* (K): In line with the host survival data (Fig. 1), we found more
319 CFU of this pathogen the older the larval host was (t_{71}= 4.27, p < 0.0001). The growth
320 of K significantly decreased with higher CFU of the coinfecting B at both timepoints
321 (CFU effect of B: t_{71} = -2.48, p = 0.0156). Interestingly, our model predicts that K
322 reaches higher CFU if C is present at sufficiently high numbers (CFU effect of C: t_{71} =
323 2.90, p = 0.0050), but because C never reached high CFU itself, the overall effect of C
324 on K was negative in our experiments (main effect of C: t_{71} = -2.92, p < 0.0047).

325 *P. aeruginosa* (P): The CFU of P significantly increased from 6 to 12 hpi (t_{73} =
326 9.89, $p < 0.0001$). P growth was only affected by K, which had a strong negative impact
327 at 6 hpi (CFU effect of K: $t_{73} = -4.40$, $p < 0.0001$).

328 While the number of interactions decreased over time (58% at 6 hpi; 42% at 12
329 hpi), all interactions were negative at both timepoints. Our four bacterial species
330 spanned from being inhibited by one (P) or two other species (B, C, K) and inhibiting
331 one (B, C), two (P) or three (K) other species (Fig. 4B).

Discussion

There is increasing evidence that polymicrobial infections are common [1]–[4] and that ecological and evolutionary interactions between co-infecting pathogens can affect host morbidity [5]–[7]. In our study, we examined whether there are generalizable patterns that characterize interaction dynamics between pathogens and a common host in polymicrobial infections. For our experiments, we used the larvae of *G. mellonella* as the host and infected it with four opportunistic human bacterial pathogens alone and in all possible combinations of mixed infections. We tested the rank order of virulence for the four pathogens and found that it was identical to the rank order of growth in the host. In addition, the more virulent species in mono infections were also better at outcompeting other species in mixed infections. A consequence of this was that the most virulent species determined host survival dynamics in mixed infections regardless of the number and type of pathogens mixed. Our findings, which held for all pathogen combinations tested, reveal an infection dynamic that is not covered by any of the current models for pathogen virulence in mixed infections.

While we found that the virulence of a specific pathogen is positively linked to its growth and competitiveness in the host, our co-occurrence analysis could give us an idea of the relative importance of pathogen growth versus competitiveness and how it varies across pathogen species combinations (Fig. 4). In the pathogen interaction network (Fig. 4B), the absence of an interaction suggests that differences in growth dominate a co-infection, meaning that the faster growing species simply outperformed the slower growing one. This was the case for five (6 hpi) and seven (12 hpi) out of the total twelve interactions. Conversely, the remaining seven (6 hpi) and five (12 hpi) interactions that were negative would imply that competitiveness played a more prominent role. At least two types of competition could be involved. First, the faster-growing species limits resource availability for the slow-growing species, reducing its

358 growth and survival due to starvation. Second, the more competitive species secretes
359 a toxin that directly targets and kills the less competitive species in interference
360 competition. While our results do not allow to differentiate between resource and
361 interference competition [44], it is likely that both mechanisms matter. For example, in
362 our mixed infections with K+B, and K+P, we observed that K inhibits its competitors
363 early on during the infections (6 hpi) but is outcompeted at a later stage (12 hpi).
364 Because resources are unlikely to be limited early in the infection, the inhibitory effects
365 can be explained by K secreting a toxin, while the dominance of B and P later in the
366 infection could be due to resource competition advantages. Alternatively, it could be
367 that K grows quickly but inefficiently while its competitors (B and P) grow more slowly
368 but efficiently and thus outpace K over time.

369 Important to note is also that all pathogen interactions were either negative or
370 neutral, but never positive. This finding supports the view that competition is much
371 more prevalent between bacterial species than positive interactions, where one
372 species unilaterally or mutually benefits another species [45], [46]. The prevalence of
373 competitive interactions is perhaps expected given that the pathogens interacted in a
374 closed environment (i.e., the larva), where both resource availability and host longevity
375 are limited [47].

376 Competition between pathogens is also a major component of mathematical
377 models predicting virulence levels [48]. A traditional set of models assumes that
378 genetically diverse pathogens engage in increased levels of resource competition in
379 mixed infections, which is predicted to exacerbate virulence [47]. Other models
380 examined the effect of infighting between pathogens through toxin secretion [49] or
381 competition for publicly shared virulence factors [50]. These models predict that
382 increased competition between pathogens should decrease virulence in mixed
383 infections. Empirical support for these models vary, lending support to both types of

384 predictions [51]–[54]. A key insight from these studies is that the biological details of
385 pathogen interactions matter. While our study was not designed to test specific model
386 predictions, our results put forth a third virulence scenario, namely that pathogen
387 interactions in mixed infections neither increase nor decrease virulence, but the
388 virulence trajectory simply follows that of the more harmful species. A first example of
389 this scenario was reported by Massey et al. [53] and here we reveal its generality. As
390 discussed above, this pattern can arise when pathogen traits that are relevant for
391 infections (virulence, growth, and competitiveness) are positively connected with one
392 another.

393 Our data further indicate that host factors also influence pathogen virulence
394 patterns. For example, we found that younger larvae had longer survival times than
395 older larvae when infected with B, C, and K. Given that *G. mellonella* has an innate
396 immune system similar to the one of vertebrates, our results indicate that the immune
397 response works well against weaker pathogens (like C and K) but deteriorates with
398 age. Another host effect we observed is that *G. mellonella* managed to control
399 infections of C and K at low injection doses, again highlighting the potency of the
400 insect's immune system. All these host effects vanished in infections with P, the most
401 virulent pathogen in our experiment, which seems to simply overrule host effects.
402 Clearly, host effects are important and likely feedback on pathogen-pathogen
403 interactions, which is why they should be considered in future work on polymicrobial
404 infections.

405 In conclusion, we can draw two generalities from our four-bacteria-infection
406 system. First, no matter what pathogen combination we used, the most virulent
407 pathogen dictated host survival. This indicates that targeting the most virulent
408 pathogen seems the most promising strategy to treat polymicrobial infections. Second,
409 more virulent pathogens grow better in the host and are better in competition with less

410 virulent pathogens. These observations suggest that the same traits (or co-regulated
411 traits) responsible for attacking the host (e.g., virulence factors) could promote
412 pathogen growth and help in competition with other pathogens. Identifying these traits
413 could give rise to promising strategies to control polymicrobial infections.

414 **Data availability**

415 All raw data sets will be deposited in the figshare repository (LINK).

416

417 **Supplementary information**

418 Supplementary information will be made available online: Supplemental file, XLSX file,

419 XX MB.

420

421 **Acknowledgements**

422 We thank Kayla King, Anna-Liisa Laine, Alex Hall, and Roland Regoes for their

423 scientific inputs. We also thank Nadine Koch for showing us how to conduct injections

424 with the larvae of *G. mellonella*.

425

426 **Funding**

427 This project has received funding from the Swiss National Science Foundation (grant

428 no. 31003A_182499 to RK) and from the Novartis Foundation for Medical-Biological

429 Research (to RK).

430

431 **Compliance with ethical standards**

432 Conflict of interest: The authors declare that they have no conflict of interest.

433

434 **References**

435 [1] B. M. Peters, M. A. Jabra-rizk, J. W. Costerton, and M. E. Shirtliff, "Polymicrobial

436 Interactions: Impact on Pathogenesis and Human Disease," *Clin. Microbiol.*

437 *Rev.*, vol. 25, no. 1, pp. 193–213, 2012.

438 [2] K. A. Brogden, J. M. Guthmiller, and C. E. Taylor, "Human polymicrobial

439 infections," *Lancet*, vol. 365, no. 9455, pp. 253–255, 2005.

440 [3] F. L. Short, S. L. Murdoch, and R. P. Ryan, “Polybacterial human disease: the
441 ills of social networking,” *Trends Microbiol.*, vol. 22, no. 9, pp. 508–516, 2014.
442 [4] A. Folkesson *et al.*, “Adaptation of Pseudomonas aeruginosa to the cystic
443 fibrosis airway: An evolutionary perspective,” *Nat. Rev. Microbiol.*, vol. 10, no.
444 12, pp. 841–851, 2012.
445 [5] C. Rezzoagli, E. T. Granato, and R. Kümmerli, “Harnessing bacterial interactions
446 to manage infections: a review on the opportunistic pathogen Pseudomonas
447 aeruginosa as a case example,” *J. Med. Microbiol.*, vol. 68, no. 12, pp. 1–15,
448 2019.
449 [6] A. Stacy, J. Everett, P. Jorth, U. Trivedi, K. P. Rumbaugh, and M. Whiteley,
450 “Bacterial fight-and-flight responses enhance virulence in a polymicrobial
451 infection,” *Proc. Natl. Acad. Sci. U. S. A.*, vol. 111, no. 21, pp. 7819–7824, 2014.
452 [7] A. Korgaonkar, U. Trivedi, K. P. Rumbaugh, and M. Whiteley, “Community
453 surveillance enhances Pseudomonas aeruginosa virulence during polymicrobial
454 infection,” *Proc. Natl. Acad. Sci. U. S. A.*, vol. 110, no. 3, pp. 1059–1064, 2013.
455 [8] S. A. Frank, “Models of plant-pathogen coevolution,” *Trends Genet.*, vol. 8, no.
456 6, pp. 213–219, 1992.
457 [9] S. A. Frank, “Coevolutionary genetics of plants and pathogens,” *Evol. Ecol.*, vol.
458 7, no. 1, pp. 45–75, 1993.
459 [10] M. Van Baalen, “Coevolution of recovery ability and virulence,” *Proc. R. Soc.*
460 *London B*, vol. 265, no. 1393, pp. 317–325, 1998.
461 [11] A. Buckling and P. B. Rainey, “Antagonistic coevolution between a bacterium
462 and a bacteriophage,” *Proc. R. Soc. London B*, vol. 269, no. 1494, pp. 931–936,
463 2002.
464 [12] A. Nourmohammad, J. Otwinowski, and J. B. Plotkin, “Host-Pathogen
465 Coevolution and the Emergence of Broadly Neutralizing Antibodies in Chronic

466 Infections," *PLoS Genet.*, vol. 12, no. 7, pp. 1–23, 2016.
467 [13] A. Papkou *et al.*, "The genomic basis of red queen dynamics during rapid
468 reciprocal host–pathogen coevolution," *Proc. Natl. Acad. Sci. U. S. A.*, vol. 116,
469 no. 3, pp. 923–928, 2019.
470 [14] D. H. Limoli and L. R. Hoffman, "Help, hinder, hide and harm: What can we learn
471 from the interactions between Pseudomonas aeruginosa and Staphylococcus
472 aureus during respiratory infections?," *BMJ*, vol. 74, no. 7. pp. 684–692, 2019.
473 [15] G. Orazi, K. L. Ruoff, and G. A. O'Toole, "Pseudomonas aeruginosa Increases
474 the Sensitivity of Biofilm- Grown Staphylococcus aureus to Membrane-Targeting
475 Antiseptics and Antibiotics," *MBio*, vol. 10, no. 4, pp. 1–15, 2019.
476 [16] M. Tognon, T. Köhler, A. Luscher, and C. Van Delden, "Transcriptional profiling
477 of Pseudomonas aeruginosa and Staphylococcus aureus during in vitro co-
478 culture," *BMC Genomics*, vol. 20, no. 1, pp. 1–15, 2019.
479 [17] S. Niggli and R. Kümmerli, "Strain Background, Species Frequency, and
480 Environmental Conditions Are Important in Determining Pseudomonas
481 aeruginosa and Staphylococcus aureus Population Dynamics and Species
482 Coexistence," *Appl. Environ. Microbiol.*, vol. 86, no. 18, pp. 1–14, 2020.
483 [18] G. Sheehan, A. Garvey, M. Croke, and K. Kavanagh, "Innate humoral immune
484 defences in mammals and insects: The same, with differences?," *Virulence*, vol.
485 9, no. 1, pp. 1625–1639, 2018.
486 [19] C. J. Y. Tsai, J. M. S. Loh, and T. Proft, "Galleria mellonella infection models for
487 the study of bacterial diseases and for antimicrobial drug testing," *Virulence*, vol.
488 7, no. 3, pp. 214–229, 2016.
489 [20] N. Ramarao, C. Nielsen-Leroux, and D. Lereclus, "The insect Galleria mellonella
490 as a powerful infection model to investigate bacterial pathogenesis.," *J. Vis. Exp.
491 JoVE*, no. 70, pp. 1–7, 2012.

492 [21] J. C. Junqueira, “Galleria mellonella as a model host for human pathogens:
493 Recent studies and new perspectives,” *Virulence*, vol. 3, no. 6, pp. 474–476,
494 2012.
495 [22] J. Revuz *et al.*, “Toxic Epidermal Necrolysis,” *Arch. Dermatol.*, vol. 123, no. 9,
496 pp. 1160–1165, 1987.
497 [23] R. Gaynes and J. R. Edwards, “Overview of nosocomial infections caused by
498 gram-negative bacilli,” *Clin. Infect. Dis.*, vol. 41, no. 6, pp. 848–854, 2005.
499 [24] P. Vandamme *et al.*, “Occurrence of Multiple Genomovars of Burkholderia
500 cepacia in Cystic Fibrosis Patients and Proposal of Burkholderia multivorans sp
501 . nov .,” *Int. J. Syst. Bacteriol.*, vol. 47, no. 4, pp. 1188–1200, 1997.
502 [25] J. Yang, H. Long, Y. Hu, Y. Feng, A. McNally, and Z. Zong, “Klebsiella oxytoca
503 Complex: Update on Taxonomy, Antimicrobial Resistance, and Virulence,” *Clin.*
504 *Microbiol. Rev.*, vol. 35, no. 1, 2022.
505 [26] R. Podschun and U. Ullmann, “Klebsiella spp. as nosocomial pathogens:
506 Epidemiology, taxonomy, typing methods, and pathogenicity factors,” *Clin.*
507 *Microbiol. Rev.*, vol. 11, no. 4, pp. 589–603, 1998.
508 [27] C. Högenauer *et al.*, “Klebsiella oxytoca as a Causative Organism of Antibiotic-
509 Associated Hemorrhagic Colitis,” *N. Engl. J. Med.*, vol. 355, no. 23, pp. 2418–
510 26, 2006.
511 [28] N. Neog, U. Phukan, M. Puzari, M. Sharma, and P. Chetia, “Klebsiella oxytoca
512 and Emerging Nosocomial Infections,” *Curr. Microbiol.*, vol. 78, no. 4, pp. 1115–
513 1123, 2021.
514 [29] C. Iversen *et al.*, “The taxonomy of Enterobacter sakazakii: Proposal of a new
515 genus Cronobacter gen. nov. and descriptions of Cronobacter sakazakii comb.
516 nov. Cronobacter sakazakii subsp. sakazakii, comb. nov., Cronobacter sakazakii
517 subsp. malonaticus subsp. nov., ...,” *BMC Evol. Biol.*, vol. 7, no. 64, pp. 1–11,

518 2007.
519 [30] J. R. W. Govan and V. Deretic, “Microbial pathogenesis in cystic fibrosis: Mucoid
520 Pseudomonas aeruginosa and Burkholderia cepacia,” *Microbiol. Rev.*, vol. 60,
521 no. 3, pp. 539–574, 1996.
522 [31] L. Eberl and B. Tümmler, “Pseudomonas aeruginosa and Burkholderia cepacia
523 in cystic fibrosis: Genome evolution, interactions and adaptation,” *Int. J. Med.*
524 *Microbiol.*, vol. 294, no. 2–3, pp. 123–131, 2004.
525 [32] H. A. Abbas, E. M. El-Masry, and G. H. Shaker, “Bacterial Etiology and
526 Antimicrobial Resistance of,” *Int. J. Biol. Pharm. Res.*, vol. 4, no. 12, pp. 1251–
527 1255, 2013.
528 [33] O. A. Forson, E. Ayanka, M. Olu-Taiwo, P. J. Pappoe-Ashong, and P. J. Ayeh-
529 Kumi, “Bacterial infections in burn wound patients at a tertiary teaching hospital
530 in Accra, Ghana.,” *Ann. Burns Fire Disasters*, vol. 30, no. 2, pp. 116–120, 2017.
531 [34] C. K. Stover *et al.*, “Complete genome sequence of Pseudomonas aeruginosa
532 PAO1, an opportunistic pathogen,” *Nature*, vol. 406, no. 6799, pp. 959–964,
533 2000.
534 [35] E. Mahenthiralingam *et al.*, “Diagnostically and experimentally useful panel of
535 strains from the Burkholderia cepacia complex,” *J. Clin. Microbiol.*, vol. 38, no.
536 2, pp. 910–913, 2000.
537 [36] A. Andrea, K. A. Krogfelt, and H. Jenssen, “Methods and challenges of using the
538 greater wax moth (Galleria mellonella) as a model organism in antimicrobial
539 compound discovery,” *Microorganisms*, vol. 7, no. 3, pp. 1–9, 2019.
540 [37] B. Y. Peng *et al.*, “Biodegradation of Polystyrene by Dark (Tenebrio obscurus)
541 and Yellow (Tenebrio molitor) Mealworms (Coleoptera: Tenebrionidae),”
542 *Environ. Sci. Technol.*, vol. 53, no. 9, pp. 5256–5265, 2019.
543 [38] C. N. Allonsius, W. Van Beeck, I. De Boeck, S. Wittouck, and S. Lebeer, “The

544 microbiome of the invertebrate model host Galleria mellonella is dominated by
545 Enterococcus," *Anim. Microbiome*, vol. 1, no. 1, pp. 1–7, 2019.
546 [39] R Core Team, "R: A language and environment for statistical computing." R
547 foundation for statistical computing, Vienna, Austria, 2021.
548 [40] T. M. Therneau and P. M. Grambsch, "Modeling Survival Data: Extending the
549 Cox Model." Springer, New York, 2000.
550 [41] C. Ritz, F. Baty, J. C. Streibig, and D. Gerhard, "Dose-Response Analysis Using
551 R," *PLoS One*, vol. 10, no. 12, p. e0146021, 2015.
552 [42] S. Mangiafico, "rcompanion: Functions to Support Extension Education Program
553 Evaluation. R package version 2.4.1," vol. 10. p. 146021, 2021.
554 [43] A.-N. Spiess, "propagate: Propagation of Uncertainty. R package version 1.0-6."
555 2018.
556 [44] M. Ghoul and S. Mitri, "The Ecology and Evolution of Microbial Competition,"
557 *Trends Microbiol.*, vol. 24, no. 10, pp. 833–845, 2016.
558 [45] N. M. Oliveira, R. Niehus, and K. R. Foster, "Evolutionary limits to cooperation in
559 microbial communities," *Proc. Natl. Acad. Sci. U. S. A.*, vol. 111, no. 50, pp.
560 17941–17946, 2014.
561 [46] K. R. Foster and T. Bell, "Competition, not cooperation, dominates interactions
562 among culturable microbial species," *Curr. Biol.*, vol. 22, no. 19, pp. 1845–1850,
563 2012.
564 [47] S. A. Frank, "Models of Parasite Virulence Steven," *Q. Rev. Biol.*, vol. 71, no. 1,
565 pp. 37–78, 1996.
566 [48] A. Buckling and M. A. Brockhurst, "Kin selection and the evolution of virulence,"
567 *Heredity (Edinb).*, vol. 100, no. 5, pp. 484–488, 2008.
568 [49] R. F. Inglis, A. Gardner, P. Cornelis, and A. Buckling, "Spite and virulence in the
569 bacterium Pseudomonas aeruginosa," *Proc. Natl. Acad. Sci.*, vol. 106, no. 14,

570 pp. 5703–5707, 2009.

571 [50] S. A. West and A. Buckling, “Cooperation , virulence and siderophore production
572 in bacterial parasites,” *Proc. R. Soc. London B*, vol. 270, no. 1510, pp. 37–44,
573 2003.

574 [51] A. F. Read and L. H. Taylor, “The Ecology of Genetically Diverse Infections,”
575 *Science (80-.).*, vol. 292, no. 5519, pp. 1099–1103, 2001.

576 [52] E. T. Granato, C. Ziegenhain, R. L. Marvig, and R. Kümmerli, “Low spatial
577 structure and selection against secreted virulence factors attenuates
578 pathogenicity in Pseudomonas aeruginosa,” *ISME J.*, vol. 12, no. 12, pp. 2907–
579 2918, 2018.

580 [53] R. C. Massey, A. Buckling, and R. Ffrench-Constant, “Interference competition
581 and parasite virulence,” *Proc. R. Soc. London B*, vol. 271, pp. 785–788, 2004.

582 [54] M. Boots and M. Mealor, “Local Interactions Select for Lower Pathogen
583 Infectivity,” *Science*, vol. 315, no. 5816, pp. 1284–1286, 2007.

584

585 **Figures**

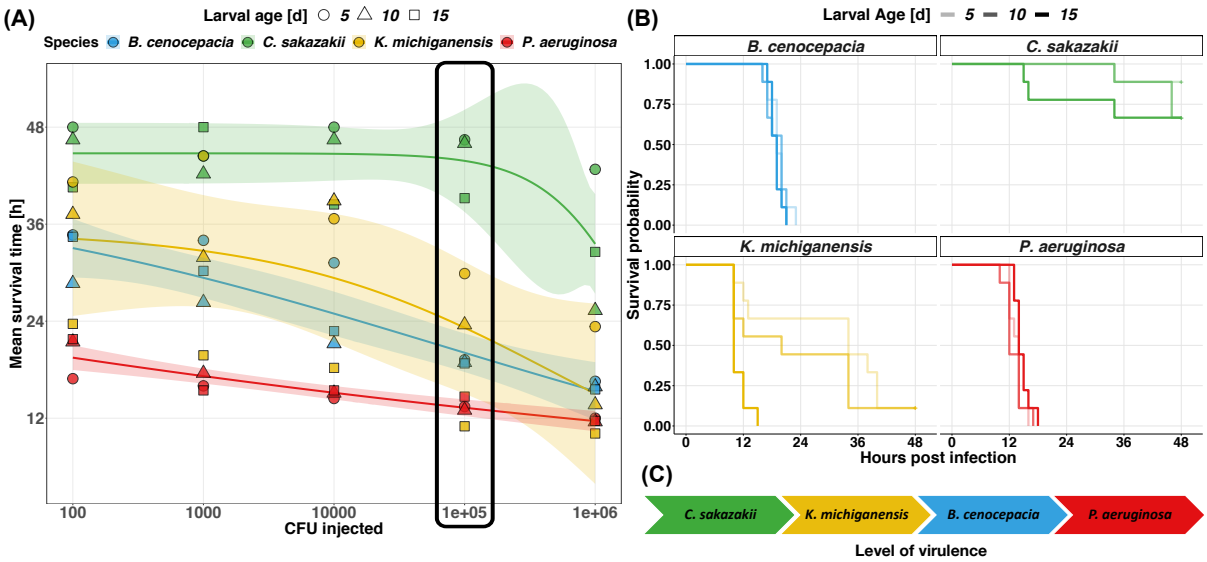

586

587 **Figure 1.** Survival rates of greater wax moth larvae (G. mellonella) are affected by the
588 pathogen species they are infected with, injection dose, and larval age. (A) Mean
589 survival time of G. mellonella larvae (measured as the area under the full survival
590 curve) as a function of larval age (5, 10, 15 days), injection dose (CFU = colony forming
591 units), and pathogen species (blue: B. cenocepacia, green: C. sakazakii, yellow: K.
592 michiganensis, red: P. aeruginosa). The lines and the shaded area (95% CI) depict the
593 relationship between mean survival time (across the different larval ages and
594 replicates) and infection dose for each species. The black box highlights the injection
595 dose chosen for all subsequent experiments. (B) Kaplan Meier survival curves of G.
596 mellonella larvae for an injection dose of 10^5 CFU for each of the four pathogen
597 species. Larval age – 5, 10, and 15 days old – is indicated by increasing line
598 opaqueness. (C) The arrow chart shows the order of virulence level among the four
599 bacterial pathogens, from lowest to highest based on our experimental data. Data are
600 from three independent experiments, each featuring 10-12 larvae per treatment,
601 resulting in a total of 30-36 larvae per treatment.

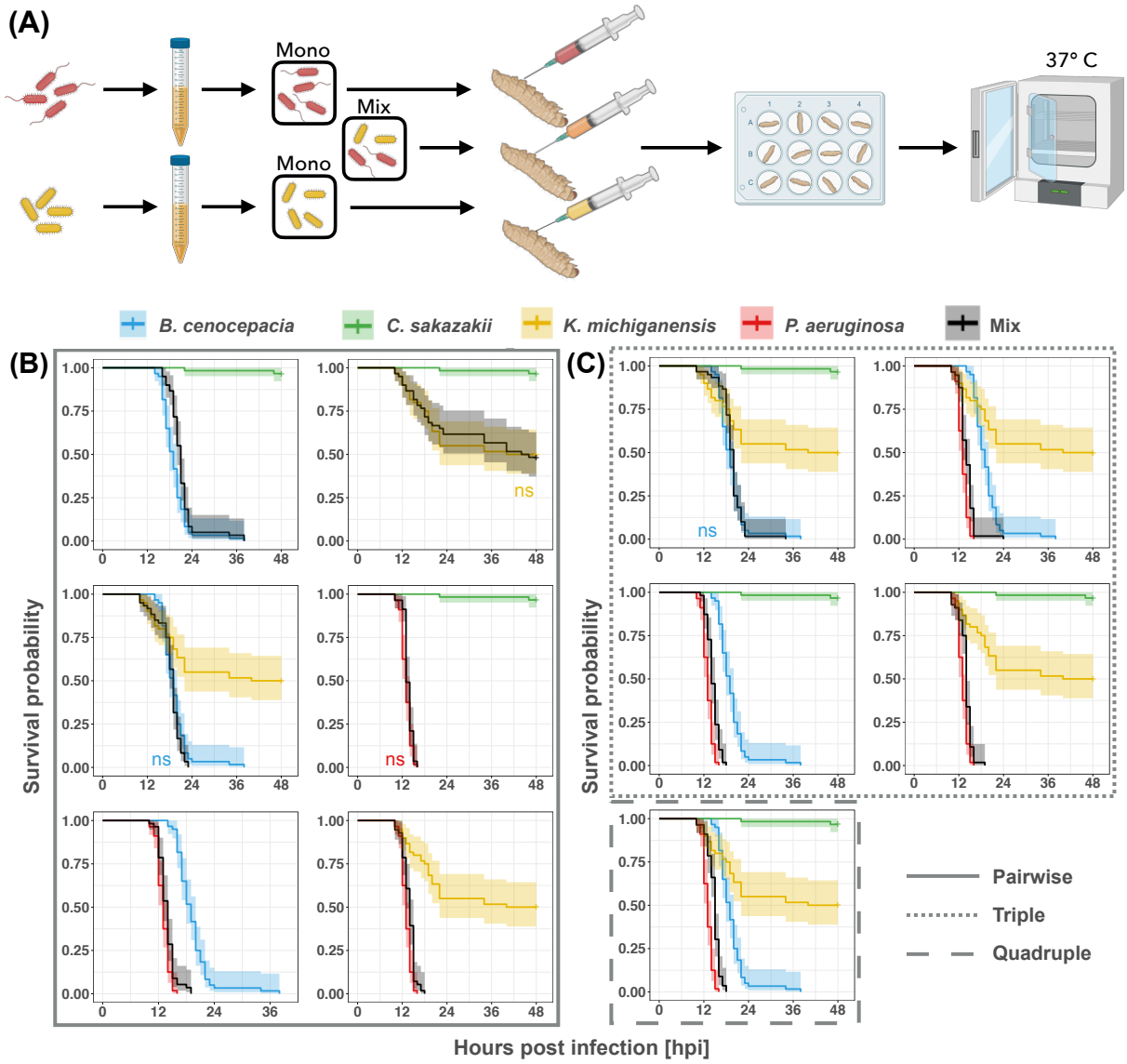

Figure 2. Host survival dynamics of *G. mellonella* larvae of pairwise, triple, and quadruple bacterial infections follow the pattern of the mono infection of the most virulent pathogen in a mix. (A) Schematic overview of the experimental setup with the example of the mono and pairwise infections of *P. aeruginosa* (red) and *K. michiganensis* (yellow). A total of 10^5 CFU was injected into G. mellonella larvae with equal amounts of each species in a mix. Kaplan Meier survival curves of mono (respective colored curves) versus pairwise (B), triple, and quadruple (C) (black curves) infections with the shaded area indicating the 95% CI. The denotation ns (non-significance) marks cases for which survival does not significantly differ between the mono infection of the colored pathogen compared to the black mix in the same panel. In all other cases, we found significant differences. Data are from five independent experiments, each with 10-12 larvae per treatment, resulting in a total of 50-60 larvae per treatment.

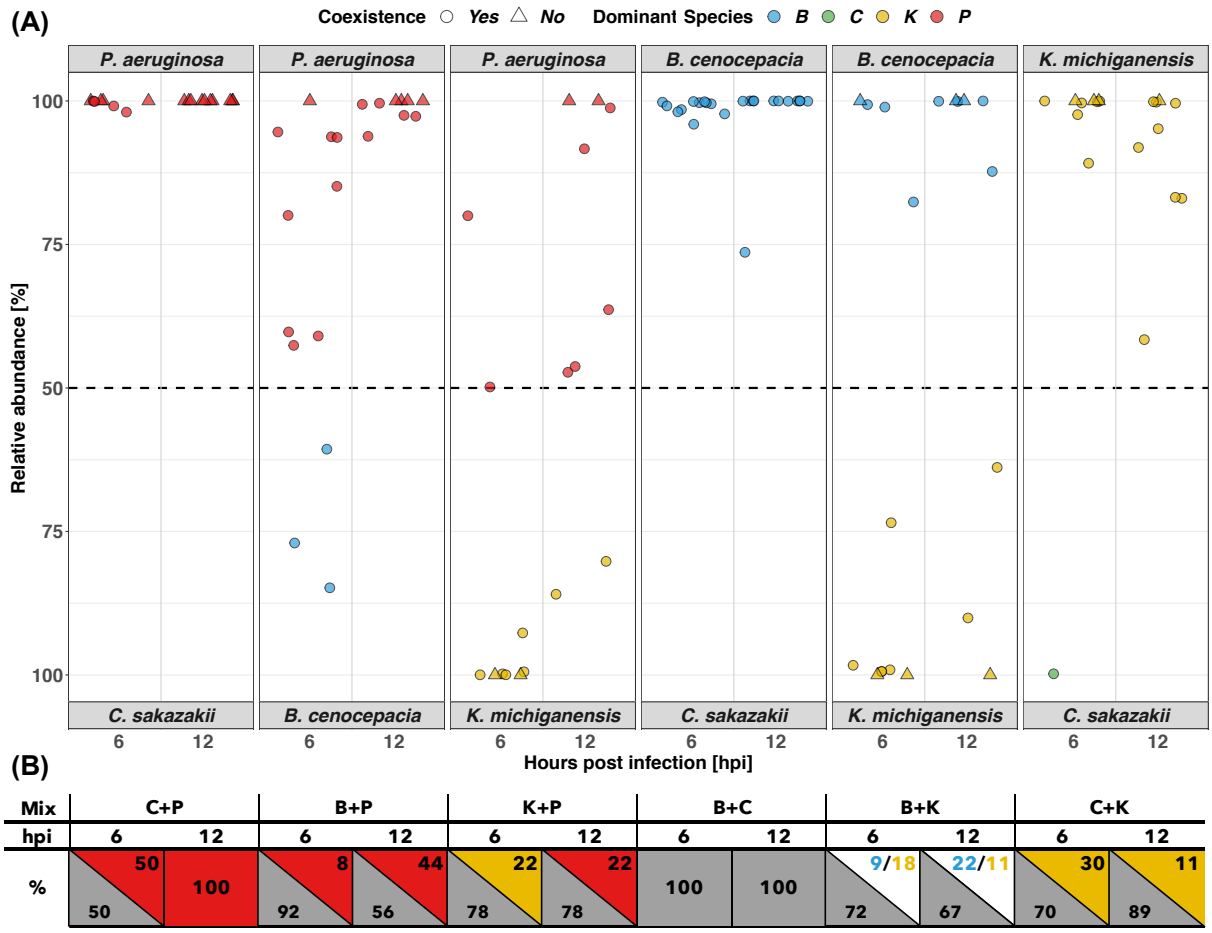

Figure 3. The more virulent pathogen is more abundant in pairwise infections and coexistence is present for five out of six pairings throughout the infection. (A) Relative abundance in pairwise infections of *G. mellonella* larvae at 6 and 12 hours post infection (hpi). The panels follow the order of the more virulent species in the mix, from left to right, with the more virulent species being indicated on top of each panel. Each datapoint represents one larva and is colored according to its more abundant pathogenic species. Circular datapoints represent pairwise infections in which both pathogens were found at 6 hpi or 12 hpi and triangles indicate datapoints for which only one of the injected species remained in the host. (B) Rectangles and triangles show the percentage of larvae in which either coexistence (grey) of pathogens occurred or only a single species (color) was left. Data are shown for all pairwise infections both at 6 hpi and 12 hpi. Values of 100% in panel A highlight larvae in which the rarer species was either no longer present or below the detection limit. Data are from 4-5 individual experiments with 2-3 larvae per treatment, resulting in a total of 8-12 larvae per treatment.

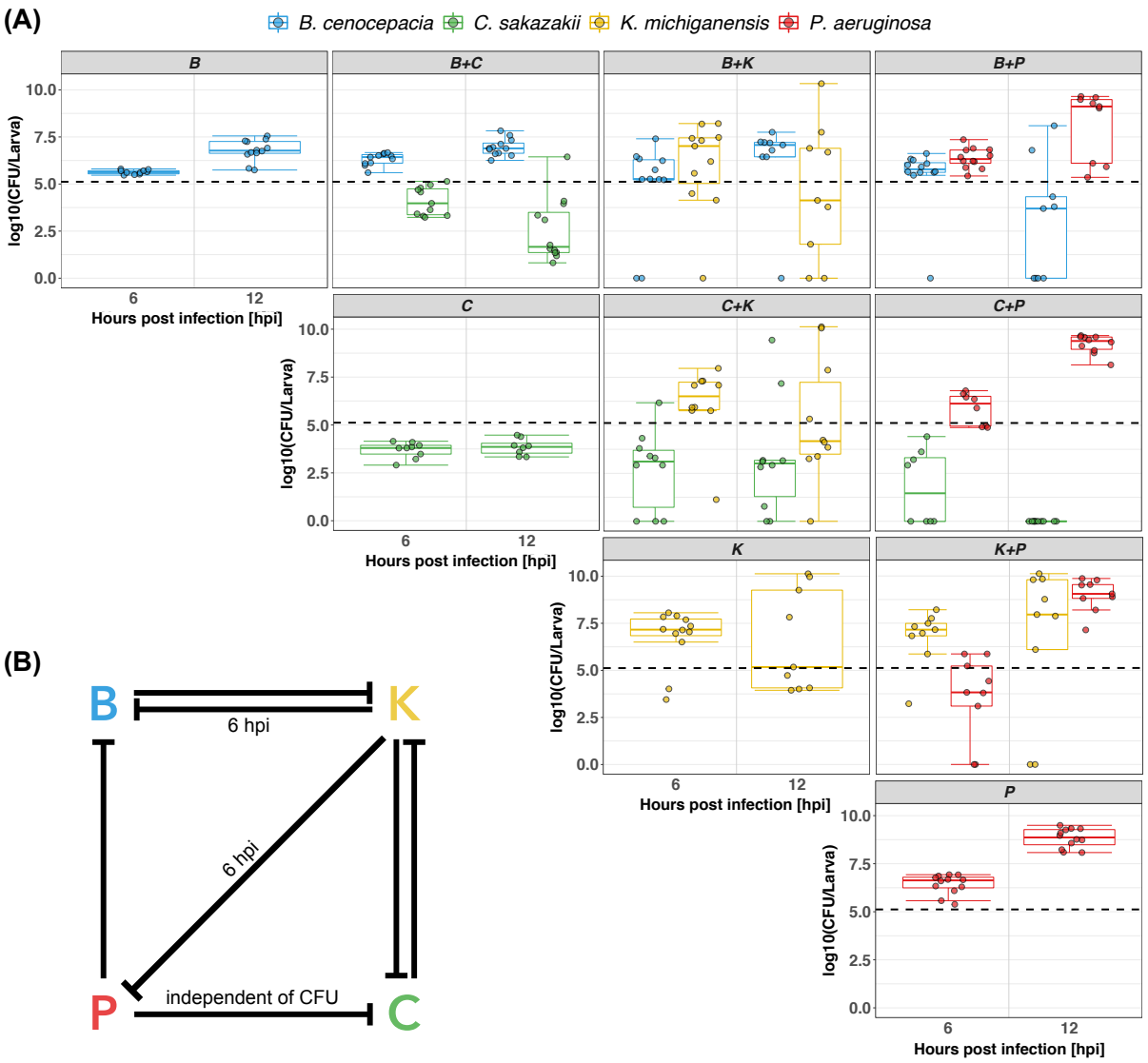

632

633 **Figure 4.** Bacterial load in *G. mellonella* larvae infected with a single pathogen or pairs
634 of pathogens 6 and 12 hours post infection (hpi). (A) Boxplots depict the number of
635 colony forming units (CFU) per larva for the mono infections of B, C, K, and P, and all
636 pairwise infections for the two time points measured. Dots represent data from
637 individual larvae. The dashed black line shows the injection dose of 50 000 CFU per
638 species in mixed infections. The dose for mono infections was 100 000 CFU. To be
639 able to directly compare the CFU between mono and mixed infections, we halved the
640 actual CFU counts obtained from the mono infections. Boxplots show the median (line
641 within the box) with the first and third quartiles. The whiskers cover 1.5x of the
642 interquartile range or extend from the lowest to the highest value if all values fall within
643 the 1.5x interquartile range. Data are from 4-5 individual experiments, each featuring
644 2-3 larvae per treatment, resulting in a total of 8-12 larvae per treatment. (B) Interaction
645 network of our bacterial consortium based on the statistical analysis of the data for both
646 timepoints unless indicated otherwise. Significant negative impact of one species on

647 another is depicted by a stop arrow. The label “independent of CFU” indicates that this
648 effect was not determined by the amount of the coinfecting pathogen.